AFRL-AFOSR-VA-TR-2018-0426

Ultracold Molecular Assembly and Quantum Chemistry

Kang-Kuen Ni
HARVARD COLLEGE PRESIDENT & FELLOWS OF

11/28/2018
Final Report

Air Force Research Laboratory
AF Office Of Scientific Research (AFOSR)/ RTB1
Arlington, Virginia 22203
Air Force Materiel Command

REPORT DOCUMENTATION PAGE	*Form Approved* *OMB No. 0704-0188*

1. REPORT DATE *(DD-MM-YYYY)* 10/29/2018	**2. REPORT TYPE** Final	**3. DATES COVERED** *(From - To)* 8/1/15-7/31/18

4. TITLE AND SUBTITLE Ultracold Molecular Assembly and Quantum Chemistry	**5a. CONTRACT NUMBER** n/a
	5b. GRANT NUMBER FA9550-15-1-0260
	5c. PROGRAM ELEMENT NUMBER n/a
6. AUTHOR(S) Kang-Kuen Ni	**5d. PROJECT NUMBER** n/a
	5e. TASK NUMBER n/a
	5f. WORK UNIT NUMBER n/a
7. PERFORMING ORGANIZATION NAME(S) AND ADDRESS(ES) President and Fellows of Harvard College 1033 Massachusetts Avenue Cambridge, MA 02138	**8. PERFORMING ORGANIZATION REPORT NUMBER** n/a
9. SPONSORING/MONITORING AGENCY NAME(S) AND ADDRESS(ES) Air Force Office of Scientific Research 875 NORTH RANDOLPH STREET ARLINGTON VA 22203-1954	**10. SPONSOR/MONITOR'S ACRONYM(S)** AFOSR
	11. SPONSOR/MONITOR'S REPORT NUMBER(S) n/a

12. DISTRIBUTION/AVAILABILITY STATEMENT

Approved for public release

13. SUPPLEMENTARY NOTES

14. ABSTRACT

15. SUBJECT TERMS

16. SECURITY CLASSIFICATION OF:			**17. LIMITATION OF ABSTRACT**	**18. NUMBER OF PAGES**	**19a. NAME OF RESPONSIBLE PERSON**
a. REPORT	**b. ABSTRACT**	**c. THIS PAGE**			Kang-Kuen Ni
U	U	U	SAR		**19b. TELEPHONE NUMBER** *(Include area code)* 617-496-3199

DISTRIBUTION A: Distribution approved for public release.

INSTRUCTIONS FOR COMPLETING SF 298

1. REPORT DATE. Full publication date, including day, month, if available. Must cite at least the year and be Year 2000 compliant, e.g. 30-06-1998; xx-06-1998; xx-xx-1998.

2. REPORT TYPE. State the type of report, such as final, technical, interim, memorandum, master's thesis, progress, quarterly, research, special, group study, etc.

3. DATE COVERED. Indicate the time during which the work was performed and the report was written, e.g., Jun 1997 - Jun 1998; 1-10 Jun 1996; May - Nov 1998; Nov 1998.

4. TITLE. Enter title and subtitle with volume number and part number, if applicable. On classified documents, enter the title classification in parentheses.

5a. CONTRACT NUMBER. Enter all contract numbers as they appear in the report, e.g. F33315-86-C-5169.

5b. GRANT NUMBER. Enter all grant numbers as they appear in the report. e.g. AFOSR-82-1234.

5c. PROGRAM ELEMENT NUMBER. Enter all program element numbers as they appear in the report, e.g. 61101A.

5e. TASK NUMBER. Enter all task numbers as they appear in the report, e.g. 05; RF0330201; T4112.

5f. WORK UNIT NUMBER. Enter all work unit numbers as they appear in the report, e.g. 001; AFAPL30480105.

6. AUTHOR(S). Enter name(s) of person(s) responsible for writing the report, performing the research, or credited with the content of the report. The form of entry is the last name, first name, middle initial, and additional qualifiers separated by commas, e.g. Smith, Richard, J, Jr.

7. PERFORMING ORGANIZATION NAME(S) AND ADDRESS(ES). Self-explanatory.

8. PERFORMING ORGANIZATION REPORT NUMBER. Enter all unique alphanumeric report numbers assigned by the performing organization, e.g. BRL-1234; AFWL-TR-85-4017-Vol-21-PT-2.

9. SPONSORING/MONITORING AGENCY NAME(S) AND ADDRESS(ES). Enter the name and address of the organization(s) financially responsible for and monitoring the work.

10. SPONSOR/MONITOR'S ACRONYM(S). Enter, if available, e.g. BRL, ARDEC, NADC.

11. SPONSOR/MONITOR'S REPORT NUMBER(S). Enter report number as assigned by the sponsoring/ monitoring agency, if available, e.g. BRL-TR-829; -215.

12. DISTRIBUTION/AVAILABILITY STATEMENT. Use agency-mandated availability statements to indicate the public availability or distribution limitations of the report. If additional limitations/ restrictions or special markings are indicated, follow agency authorization procedures, e.g. RD/FRD, PROPIN, ITAR, etc. Include copyright information.

13. SUPPLEMENTARY NOTES. Enter information not included elsewhere such as: prepared in cooperation with; translation of; report supersedes; old edition number, etc.

14. ABSTRACT. A brief (approximately 200 words) factual summary of the most significant information.

15. SUBJECT TERMS. Key words or phrases identifying major concepts in the report.

16. SECURITY CLASSIFICATION. Enter security classification in accordance with security classification regulations, e.g. U, C, S, etc. If this form contains classified information, stamp classification level on the top and bottom of this page.

17. LIMITATION OF ABSTRACT. This block must be completed to assign a distribution limitation to the abstract. Enter UU (Unclassified Unlimited) or SAR (Same as Report). An entry in this block is necessary if the abstract is to be limited.

Ultracold Molecular Assembly and Quantum Chemistry

Kang-Kuen Ni

Department of Chemistry and Chemical Biology, Harvard University

(Dated: October 29, 2018)

Abstract

For the YIP award, I proposed to assemble single ultracold molecules, where all quantum degrees of freedom are controlled, from individually trapped atoms in the gas phase. These individual molecules are like "Lego pieces" that can be assembled to construct more complex systems. The meticulous work to control all quantum degrees of freedom and the preparation of these molecules at the lowest possible energy allows these "Lego pieces" to follow rules of quantum mechanics, which are the underlying laws of atoms and molecules. By constructing complex systems from simple building blocks where their interactions are controlled and manipulated in the quantum regime, we aim to ultimately quantum simulate and compute complex systems for applications in chemistry. Another goal utilizing these novel sources of single molecules is to study chemical reactions in the full quantum regime and to prepare the exact number of reagents participated, which will allow us to unambiguously identify the nature of the reactions. During the award period, we demonstrated making one molecules from two atoms. We built an apparatus and devised many new techniques to allow two different species (cesium and sodium) of single atoms to be trapped, cooled, and transported in optical tweezers. We studied collision in a new regime where the number of collisional partners are prepared exactly. To coherently convert a pair of atoms into a diatomic molecule, we gained control of the quantum motion of individual Cs and Na by Raman sideband ground-state cooling. We achieve cooling outside of the so called Lamb-Dicke regime, which is a new regime from what has been demonstrated previously. After gaining motional control of individual atoms, a Cs and a Na atoms are merged into the same tweezers while maintaining them in their ground states. With full quantum control of atoms achieved, we demonstrate (preliminary) coherent creation of single molecules in the vibrational least bound state of an electronic ground state. This work provides an exciting new quantum resource for simulations and information processing and a new paradigm to study chemical reactions with the exact number of reactants prepared.

I. SUMMARY

A variety of modern technological challenges can be addressed by harnessing individual molecules at the quantum level.

1) Quantum chemistry. In large thermodynamic ensembles, many reaction channels contribute, obscuring the precise chemical reaction dynamics. Single molecule control would allow us to initialize chemical reactions in a single reaction channel. This will lead to the most fundamental understanding of chemical reactions which may help with optimizing chemical synthesis processes.

2) Quantum computing. Polar molecules, with an electric dipole moment, are nature's pre-packaged "perfect qubit", furnished with internal degrees of freedom for robust storage of quantum information, as well as the long-range interactions necessary for quantum logic. Achieving the ultimate control of molecules enables us to unlock these degrees of freedom for quantum computing.

3) Quantum simulation. For similar reasons as (2), arrays of polar molecules can allow us to build up simulated quantum materials one particle at a time, then dynamically tune the atomic scale properties in real-time and study the properties of the resulting material.

Quantum control of single molecules begins with single atoms. We leverage the pioneering work over the past two decades using optical tweezers to trap and manipulate single atoms. Exquisite control of light intensity and wavefront phase enables the tweezer traps to be shaped and steered in space within a few microseconds. The tight tweezer confinement defines the atom location in space, facilitates quantum control of atomic motion, and serves as an ideal beaker for holding precisely determined number of atoms in close proximity so they can bind into a molecule. The choice of wavelength allows us to trap some species but not others. These three degrees of control afforded by optical tweezers (spatial, temporal, and atomic species) make them ideal for manipulating single atoms.

For our work, we choose the sodium cesium molecule (NaCs) because of its strong dipole moment, and because its constituent atoms, Na and Cs, can be laser-cooled with standard techniques.

Following the seminal work [1], we built the first dual-species optical tweezer system. We loaded single Na and Cs atoms from a dual-species magneto-optical trap (MOT) into separate tweezers of different wavelengths to differentiate the two species. Loading and imaging Na, which has unfavourable internal structure, necessitated a new optical tweezer technique which we demonstrated for the first time [2]. We were able to image single Na and Cs atoms, confirming for the first time co-trapping of a single Na and Cs atom side-by side in separate tweezers.

Going into the quantum regime, we achieved the best motional state control of a single Cs atom to date using Raman sideband cooling, previously demonstrated in Rubidium atoms [3, 4]. We generalized this technique to unfavourable species and demonstrated our new technique on Na [5]. We moved the Cs tweezer to the Na tweezer over a distance of 100× the spatial extent of the Cs atomic wavefunction, without exciting any of its motion. Thus, we demonstrated the persistence of quantum control of atomic motion over large distances.

After merging the two atoms into the same tweezer, we performed collisional studies between exactly two atoms, demonstrating how the optical tweezer platform could be used to isolate individual atomic collision channels [6]. It also enabled the first on-demand chemical reaction between two atoms in the gas phase which provided spectroscopic lines of NaCs [6] crucial for the next step.

We are currently working on the theory and coherent spectroscopy to determine the molecular energy levels that will serve as sequential stops on the way to the final desired molecular state, relevant for applications (2) and (3) above. We have observed and are perfecting the coherent transfer to the first of two such stops. Finally, we are also exploring techniques to generate large arrays of many tweezer-trapped molecules.

II. INTRODUCTION

Ultracold molecules offer exciting new opportunities to explore the interface of chemistry and physics. On the one hand, molecules prepared in a pure internal and external quantum state allow studies of chemical reactions fully in the quantum regime [7]. Such studies will be of fundamental importance in chemistry. On the other hand, the rich molecular internal structure and interactions allow building systems that exhibit novel quantum many-body phases [8]. Understanding and controlling fundamental chemical processes and physical interactions are central to deciphering complex systems.

Inspired by scientific and technical advances in the field of ultracold atomic and molecular physics, I proposed a new approach to assemble ultracold molecules atom-by-atom

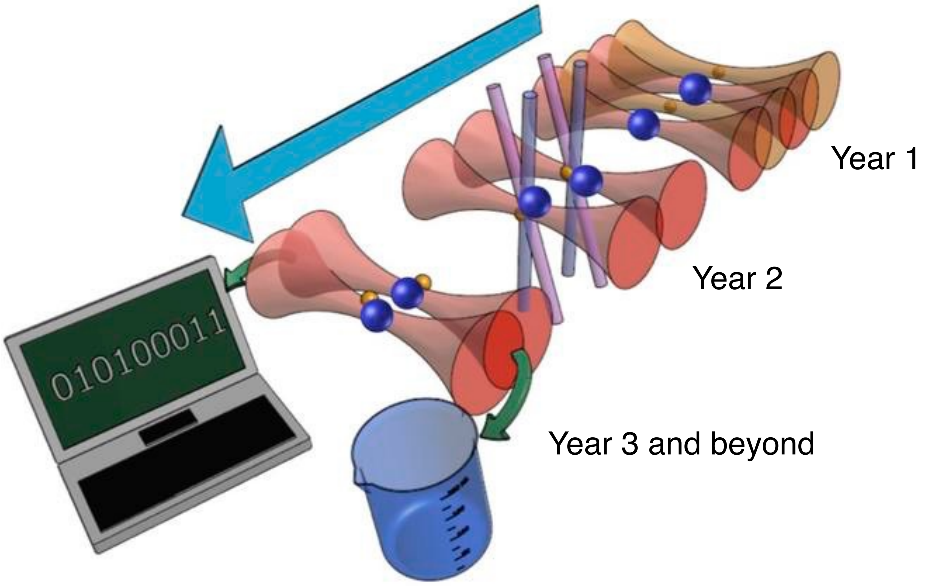

FIG. 1. **Ultracold Molecular Assembler**

and was awarded the YIP. The novel source of single gas-phase molecules would provide a new paradigm for studying chemical reactions. By preparing exactly the required number of molecules for each experimental measurement, we could unambiguously determine the species involved in a reaction. Furthermore, by combining knowledge of the initial quantum state of the reactants and the detected quantum states of the reaction products, one can learn details of the chemical reactions dynamics and elucidate the processes of bond breaking and formation. Finally, a growing number of atoms in the periodic table can be laser-cooled, which means that the first step in the proposed approach - laser cooling of atoms to ultracold temperatures - is becoming increasingly applicable. This new way of performing chemical reactions will enable the production and investigation of molecular species that would be otherwise inaccessible.

Another motivation for creating a source of single molecules is its built-in individual molecule detection and manipulation capabilities which are crucial for applications in quantum information processing and quantum simulation. Quantum computers would allow new types of calculations for chemistry [9], opening the door to quantum-computing-based discovery of molecules for medicine, energy storage, and other practical uses. Single ultracold molecules can serve as quantum bits where information can be encoded in the long-lived hyperfine or rotational states while logic gate operations utilize their long-range, tunable, and anisotropic interactions [10–12]. The single molecules can also be interfaced with strip-line microwave cavities for quantum information applications [13]. Furthermore, the same dipole-dipole interactions that give rise to gate operations can be utilized to study novel quantum phases once the system is scaled up to many molecules in a spatial configuration of one's choosing.

Many methods for trapping and cooling molecules to cold and ultracold temperatures have been demonstrated or are being pursued [14]. We follow the general approach of assembling ultracold molecules from ultracold atoms. Complete internal quantum-state control of molecules was achieved in bulk gases and optical lattices [15–22]. These advances have already opened the door to many research directions, including ultracold chemistry [23] and simulations of quantum spin models [24]. Furthermore, interesting strongly interacting phenomena can be explored with a lower entropy gas and with single molecule addressability [25, 26]. The method proposed here aims to realize both of these capabilities.

III. METHODS, ASSUMPTIONS, AND PROCEDURES - THE STEPS OF ULTRACOLD MOLECULAR ASSEMBLY

Here we outline the steps for single molecule production ("ultracold molecular assembler," see Fig. 2). This approach relies heavily on high fidelity internal and external quantum-state control of atoms and molecules and are generally applicable for a variety of species. Specifically, we chose diatomic molecules made from sodium (Na) and cesium (Cs) atoms due to their large molecular fixed-frame dipole moments (4.6 Debye) [27, 28] and extensive available spectroscopy [29–31]. For ultracold chemical reaction studies, NaCs molecules prepared in different internal states offer distinct energetic pathways to participate in chemical reactions that could be switched on and off [32].

The first step of the production (Fig. 2) is to prepare laser-cooled Na and Cs atoms in overlapped magneto-optical traps (MOTs) in a single vacuum chamber. A schematic of the apparatus is shown in Fig. 3. The MOT serves as a cold atom reservoir for loading single atoms into tightly focused optical tweezer traps [1]. When a sufficiently confined atom is illuminated with near-resonant light, a collisional blockade induces parity projection which limits the atom number to either zero or one. Loading a single atom therefore succeeds

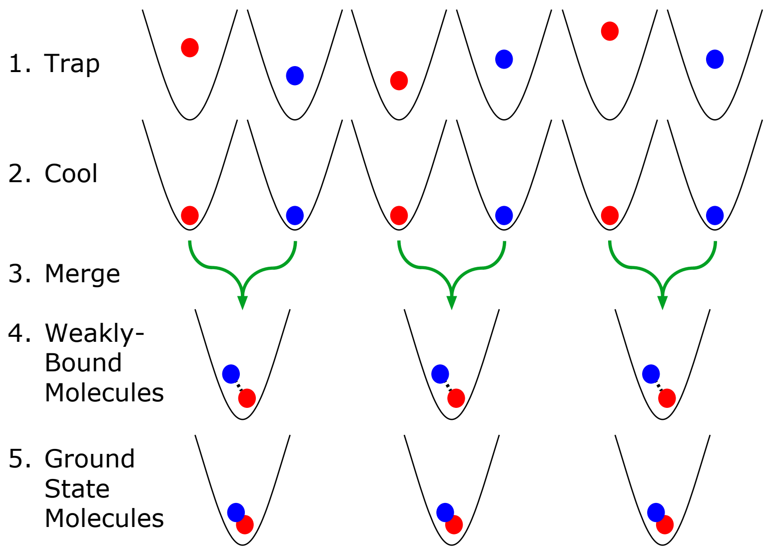

FIG. 2. **Step-by-step procedure for the "ultracold molecular assembler."** 1. Trap single atoms in adjacent optical tweezer traps. 2. Cool atoms into motional ground state. 3. Merge pair of tweezers into one. 4. Convert atom pairs into weakly-bound molecules. 5. Perform coherent internal state transfer to bring weakly-bound molecules to the rovibronic ground state.

approximately 50% of the time due to its stochastic nature [33]. To independently control Na and Cs, we choose two different color tweezers, 976 nm for Cs ($\lambda_{\mathrm{D2}} = 852$ nm) and 700 nm for Na ($\lambda_{\mathrm{D2}} = 589$ nm). The severe light shifts of Na at the trapping wavelength would normally prevent atom cooling, and consequently, efficient atom loading. We devised a way to eliminate the light shift through fast temporal alternation of trapping (tweezer) and cooling and successfully demonstrated trapping of single Na atoms [2]. This technique is general and should enable loading of other species of atoms and molecules that might otherwise experience large light shifts. Subsequently, fluorescence imaging determines if a single atom has been successfully loaded before proceeding. Simultaneous trapping of single Na and Cs atoms side-by-side was achieved in our lab, as shown in Fig. 3.

To maximize wavefunction overlap between two atoms so that they can be efficiently converted into a molecule, we desire atoms trapped in the same tweezer and with the smallest possible wavefunction spread. To achieve this, the second experimental step (Fig. 2) is to cool the atoms into their motional ground state by applying 3D Raman sideband cooling (RSC), a technique first demonstrated with single ions [34] and in more recent years with single neutral atoms [3, 4, 35]. Once Na and Cs atoms are in their 3D motional ground

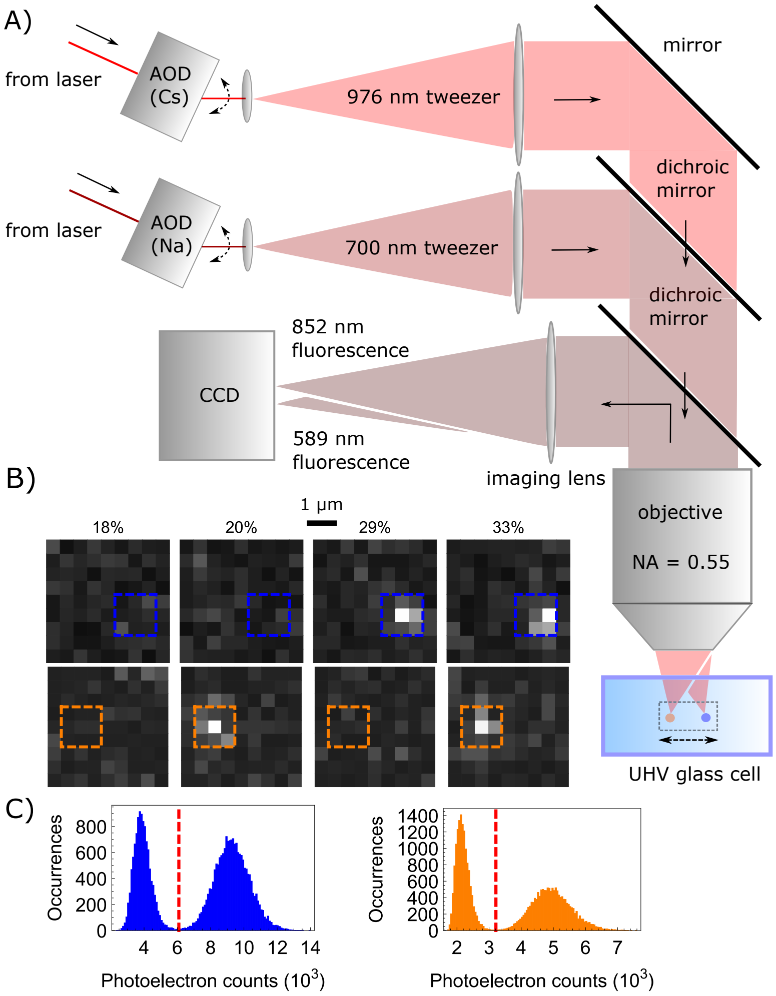

FIG. 3. **Single atom trapping. A**) Two side-by-side optical tweezers at 976nm and 700nm trap a single Cs (blue) and Na (orange) atom respectively in the vacuum chamber. Both tweezer beams are combined using a dichroic and sent through an objective. The tweezers can be scanned in the focal plane by changing the frequency of the drive for the Acousto-optic deflector (AOD) upstream in the beam path. **B**) Fluorescence images of single Na and Cs atoms. The four possible cases are shown with their initial loading probabilities: no atoms, a single Na atom, a single Cs atom, both Na and Cs atoms. **C**) Histogram of Cs (blue) and Na (orange) fluorescence. The bimodal distribution shows clear separation between zero- and one-atom peaks.

state, the two tweezers are merged. The Na tweezer trap is adiabatically ramped down to ensure that both Cs and Na are trapped at the same position.

After the two atoms are cooled to the ground state and then merged into the same trap, they are initialized in a single internal and motional quantum state. In a quadratic potential, as in the case of the bottom of an optical tweezer, two particles interacting via a delta potential can be recast into relative and center-of-mass (COM) coordinates [36]. Two atoms prepared in their respective motional quantum ground states can then be viewed as being in a single relative motional state. A pair of atoms can then be converted to a molecule in its absolute rovibrational ground state with almost unit efficiency via quantum state transfer, provided that the entire process is coherent.

The smallest wavefunction spread achievable in the confining tweezer quadratic potential corresponds to the zero-point length, $z_0 = \sqrt{\hbar/(2m\omega)}$, where m is the atomic mass, $\hbar$ is the reduced Planck's constant, and ω is the angular frequency of the trapped atom. For a representative $2\pi \times 70$ kHz trap frequency, the zero-point lengths for Na and Cs are $z_0 = 1059\,a_0$ and $z_0 = 440\,a_0$ respectively, where $a_0 = 0.053$ nm is the Bohr radius. Therefore, two atoms cooled to their motional ground state will still have an extent in one dimension more than a hundred times larger than a typical molecular bond length, making efficient conversion challenging.

To overcome technical challenges associated with bridging two quantum states with a large energy difference but small wavefunction overlap, we plan to use two steps (Fig. 2). A sodium and a cesium atom in the same tweezer will be first associated into the most weakly bound molecular state (vibrational level $\nu'' = 24$ in $a^3\Sigma^+$) by a detuned, coherent, two-photon Raman pulse. Subsequently, the weakly-bound molecule will be transferred into the rotational, vibrational, and electronic (rovibronic) ground state by STImulated Raman Adiabatic Passage (STIRAP) [37]. To check that the process is successful, residual atoms will be blown out with resonant light, and the surviving molecule will be coherently converted back into atoms for fluorescence imaging.

IV. RESULTS AND DISCUSSION

A. Building one molecules from two atoms

As a first step, we demonstrated a proof-of-principle ultracold molecular assembler (without full quantum control), which was a cover story of *Science* [6] in 2018 and captured the public's imagination.

When we think of chemistry, we usually think about making molecules, for example

$A + B \rightarrow AB$. However, in a typical chemical reaction, we start with an ensemble of A and an ensemble of B, and through stochastic encounters, some AB are made under the right condition. Going beyond this paradigm, our demonstration combines exactly two atoms into a single, controlled reaction.

We begin by trapping two individual laser-cooled atoms in separate optical tweezers and then merge the tweezers into one optical dipole trap through sending different frequencies to the beam steering acoustic-optical modulator. Once the two atoms were in the same trap, they collided frequently but could not form a molecule because the molecular binding energy is difficult to be removed without a third particle around.

To make a molecule, we applied a photo-association laser pulse to bind the atoms. The photo-association lasers were scanned for 250 GHz below an excited state atomic asymptote to form an NaCs* molecule in selected vibrational levels. The single molecule spectrum is shown in Figure 4.

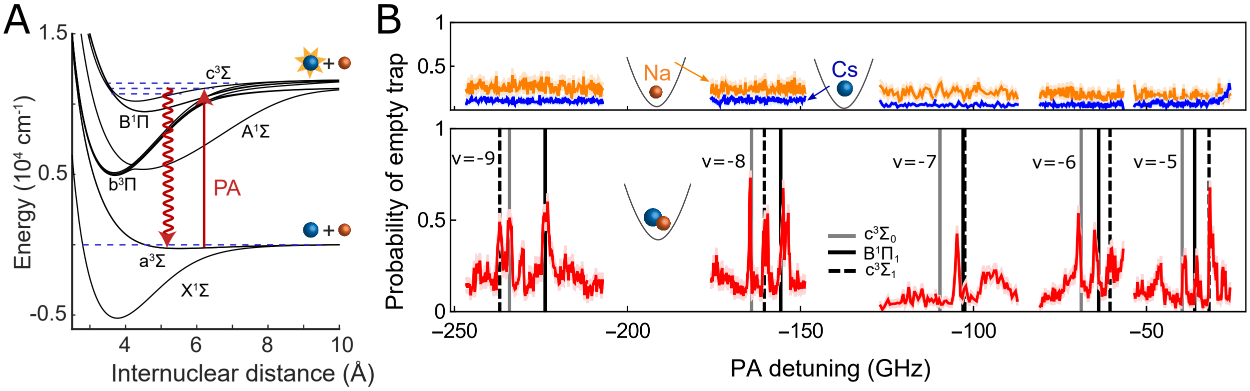

FIG. 4. (A) NaCs molecular potentials as a function of internuclear distance. Photoassociation (PA) light excites the ground state atoms to vibrational levels of the NaCs* excited molecular potentials, from which they mostly decay to vibrationally excited electronic ground state molecules (squiggly line). (B) The probability of single Na (orange), Cs (blue), and joint Na+Cs (red) atoms evolving to the "no atoms" detection channel, as the PA light. When both atoms are initially loaded into the tweezer (lower panel), 2-body loss resonances appear due to molecule formation. As a validation of our method, we check that no loss resonances are observed when only one atom is present (upper panel).

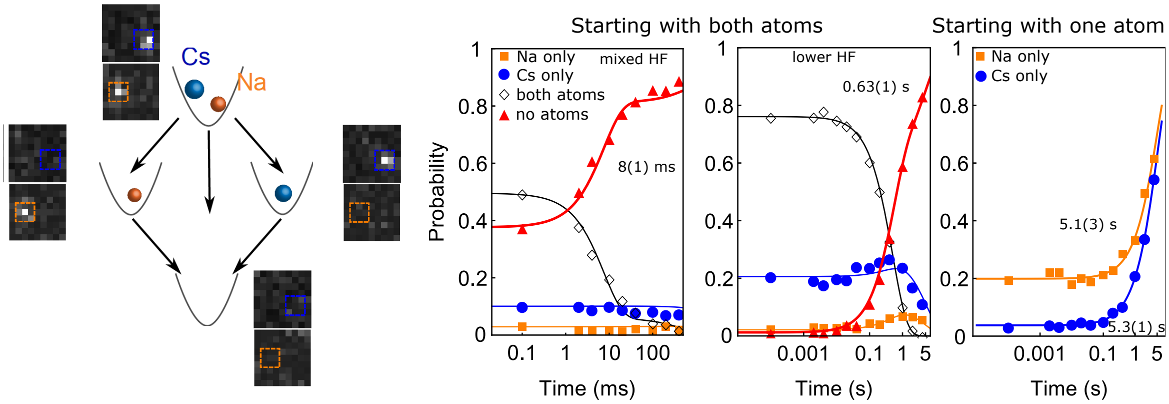

FIG. 5. **Collisions of Na and Cs.** The hold time in the merged trap is varied to measure the evolution of trap occupancy due to various collision mechanisms. Post-selection on initial and final trap occupancies allows us to distinguish 1- and 2-body processes. The fastest timescales are indicated next to the thick fitted curves. **Left**: For both atoms in a mixture of hyperfine states, the loss is dominated by rapid 2-body hyperfine-state-changing collision induced loss. **Center**: For both atoms in their lowest hyperfine states, the loss is explained by 2-body hyperfine state changing collisions that follow off-resonant scattering of trap light. In these two panels, different markers denote the final trap occupancy. **Right**: One-body loss gives background gas limited lifetime of about 5 s for both atoms. Here, we post-select on empty final tweezers and markers denote initial trap occupancy.

B. Collisions of exactly two atoms

Because we have the ability to prepare exactly two atoms in the same tight tweezer, we can study their collisions in a new regime where the exact collisional partners are prepared. As described previously, isolated collisions between two atoms do not usually result in molecule formation due to the need to simultaneously conserve momentum and energy. However, the atoms can change their hyperfine states after colliding, and the exothermic hyperfine-spin-changing collisions impart enough kinetic energy (≈ 100 mK) to the atoms to eject them from the tweezer (≈ 1 mK depth).

Generally, a given initial trap occupancy can evolve into four possible outcomes following an experiment: i) both atoms, ii) no atoms, iii) only Cs, and iv) only Na remain in the trap. Single-atom images from each repetition allow us to post-select on any of these cases and separate 1- and 2-body processes, giving both lifetimes from a single dataset (Fig. 5). For example, when Na and Cs are both present (effective pair density of $n_2 = 2\times10^{12}\,\mathrm{cm}^{-3}$ [38]), and prepared in a mixture of hyperfine spin states, they are both rapidly lost $\tau_{loss} = 8(1)\,\mathrm{ms}$, where τ_{loss} is the $1/e$ time of exponential decay. This yields a loss rate constant $\beta = 5\times10^{-11}\,\mathrm{cm}^3/\mathrm{s}$. In contrast, if the atoms are both optically pumped into the lowest energy hyperfine levels, conservation of energy prevents the change of hyperfine states, and the atom lifetime increases to 0.63(1) s, similar to the rate of hyperfine-state relaxation for Cs due to off-resonant scattering of the tweezer light [39]. When only one atom is present, 1-body loss due to collisions with background gas limits the lifetime to 5 s.

C. Full quantum control of single atoms

To maximize wavefunction overlap between two atoms so that they can be efficiently converted into a molecule, the atoms have to be trapped in the same tweezer with the smallest possible wavefunction spread. Even with the smallest possible wavefunction spread, the zero-point length z_0 in our system is a hundred times larger than a typical molecular bond length (Fig. 6). Such wave function size mismatch makes efficient conversion challenging. A key to efficiently convert atoms pairs into molecules is then to utilize coherent population transfer techniques, which requires a single quantum state preparation. For both of the above reasons, cooling single atoms into their motional ground states is a crucial next step.

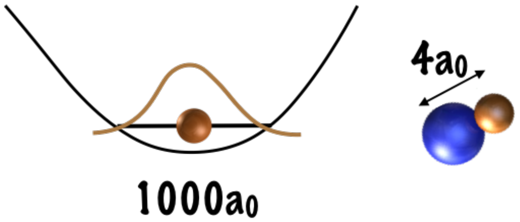

FIG. 6. The smallest wavefunction spread of an atom in an optical tweezer ($\sim 1000a_0$) is much larger than a molecular bond length $\sim 4a_0$ for NaCs. The large wavefunction mismatch illustrates the difficulty to efficiently converting an atom pair into a molecule.

Using standard MOT and polarization gradient cooling (PGC), we can cool a single Cs or Na atom to the point where the discreteness of the trap's energy levels becomes important.

To further manipulate the atom into the lowest motional state, we operate in the resolved sideband regime where the linewidth of the cooling transition is less than the trap frequency (10-100's of kHz). Raman sideband cooling (RSC) has been demonstrated for a variety of systems in this regime [3, 34, 35, 40]. We demonstrated RSC of a single Cs atom in an optical tweezer to its 3D motional ground state with population of 96(3)% (manuscript in preparation).

The challenges with RSC of sodium atoms is that the relatively high starting temperature, 70 μK prepared by optical molasses cooling, corresponds to a high starting thermal occupation number of $n_r \approx 3.4$ in the radial direction and $n_a \approx 21$ in the axial direction. Therefore, single atom population up to $n_r = 12$ and $n_a = 70$ needs to be swept to ultimately get a large population ($> 95\%$) in the ground-state ($n_r = 0$ and $n_a = 0$). The RSC consists of a motional cooling step and an optical pumping step that subsequently spontaneously emits to reset the internal state of the atom. The light mass of sodium atoms makes heating due to the spontaneous emission more pronounced. In addition, the large Lamb-Dicke parameter (the ratio comparing the zero-point spread of Na in the trap to the wavelength of addressing light) also makes preserving the motional level during the optical pumping challenging. A balance of cooling and heating determines the final ground-state population.

The cooling sequence we employed, guided by our 3D Monte-Carlo simulation, includes a few tricks. In general, the presence of a tight optical trap causes light shifts. For RSC, this implies that the optical pumping efficiency would be limited due to tensor light shifts that mix hyperfine quantum numbers. We employ a fast switching dipole trap throughout the entire RSC sequence to preserve good hyperfine quantum numbers. The optical pumping is efficient during the “off”-cycle of the switching trap. We also begin cooling sequence by addressing high order (as high as 5th-order in Fig. 7b) motional sidebands to achieve large cooling per cycle. In addition, we opt for short pulses to broaden spectrum coverage effectively eliminating anharmonicity that comes from the Gaussian trapping potential and shaped pulses to round out pulse edges to avoid carrier off-resonance excitations.

These tricks allow a single Na atom prepared in the 3D ground-state (n=0) with a population of $\sim 94\%$. Using Raman sideband spectroscopy along three different axes, 1st-order heating, 1st-order and higher-orders cooling sidebands of each axis were measured in Figure 7. The ratio of the 1st-order cooling to heating sideband height gives the fraction of the population that is not in the ground state. Hence, for each axis the ground-state population

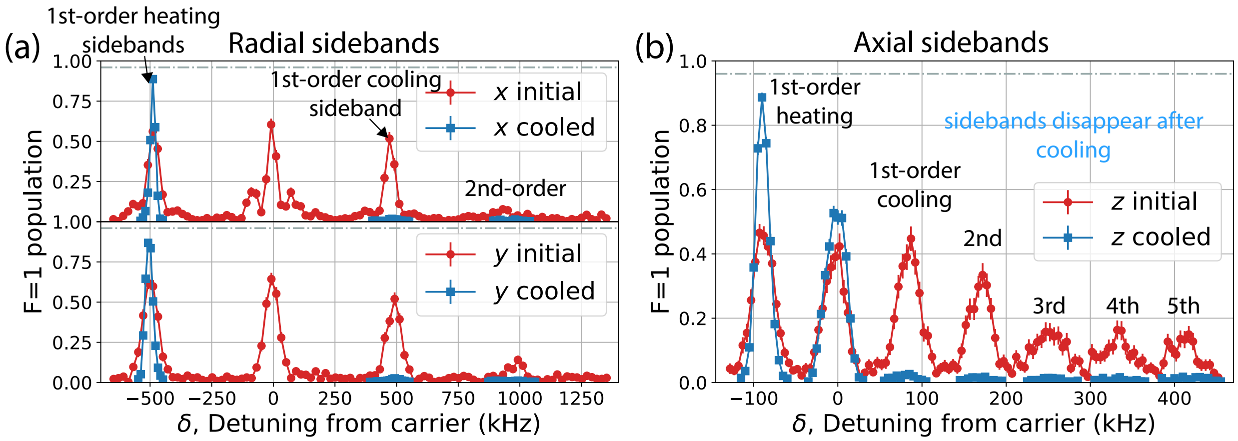

FIG. 7. Cooling of single atoms to the motional ground state. Raman sideband thermometry before and after cooling for (a) the two radial axes and (b) the weaker axial axis of a single sodium atom. The cooling sidebands are suppressed after RSC while the heating sidebands remain. The ratio of the 1st-order cooling to heating sideband height give the fraction of the population that is not in the ground state. Hence, our spectroscopy shows the ground-state population is $\sim 98\%$ for each axis after RSC. The total 3D ground-state population is achieved at $\sim 93.7\%$.

is ∼98% after RSC.

With the motional quantum degree of freedom of atoms under control, two single atoms have to be merged into the same trap for further molecule production. The locations of the two single atom traps (one at a wavelength of 700 nm and beam waist of 0.6 μm, and the other at a wavelength of 976 nm and beam waist 0.8 μm) are controlled by the deflection angles of the beams passed through two separate acoustic-optical deflectors (AOD). Figure 8 shows the merge timing sequence, the measured survivability of Na and Cs after the tweezers are overlapped, and the calculated merging trapping potentials. Due to the different polarizabilities, Na is trapped by both tweezers while Cs will see a trap and an anti-trap. During the merging process (6 ms), well depths are kept different in order to avoid bringing the motional ground and first excited state into degeneracy, which would promote atoms into the first excited state with 50% probability. Therefore, the 700 nm-tweezer is ramped down, while the 976 nm-tweezer is merged. After the two tweezers overlapped, the 700 nm-tweezer is ramped off, and both Na and Cs are trapped by the 976 nm-tweezer. As shown in Fig. 8(B), when the two tweezers are overlapped, both Na and Cs survive the merge process (the data was taken with Na and Cs not simultaneously presence for each measurement).

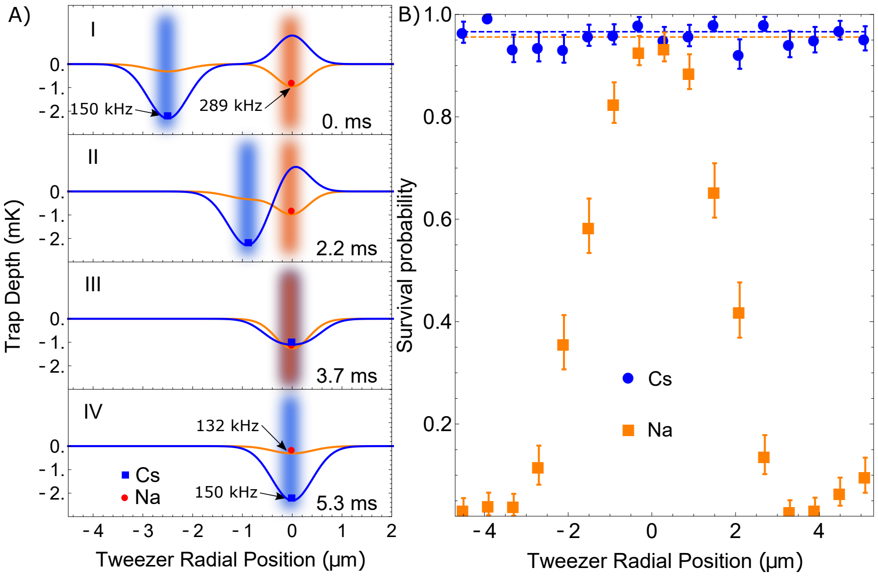

FIG. 8. **Merging single Na and Cs atoms, which are initially separated by 3 μm, into one tweezer. A**) 1-D cuts of the combined, time-varying 700 nm and 976 nm tweezer potentials for both atoms during the merge sequence. Na and Cs are represented by dots that track the minima of their potentials (orange for Na and blue for Cs). Overlaid are graphics of the optical tweezers. Radial trap frequencies are labeled in the first and last panels (axial trap frequencies are roughly 6 times smaller). Panels I-III depict the merging process. In panel IV, the 700 nm tweezer has been extinguished and only the 976 nm tweezer remains. **B**) Measured survival probability of Na and Cs after the sequence depicted in (A), followed by separating the tweezers through a reverse sequence to image the atoms. The two atoms are merged into the same tweezer at the survival maximum for Na. The dashed lines represent the survival rates due to imperfect re-imaging.

When the two tweezers are not overlapped, Na is loss because the 700nm-tweezer is completely off at the "hold" period while the 976nm-tweezer is not aligned which results in no confining potential.

D. Preliminary demonstration of coherent molecule creation

To further utilize such a novel source of single molecules for quantum simulation and quantum information processing, the molecules will be prepared in their rovibrational ground state such that they are long-lived and possess a large molecular fixed-frame dipole moment. To do so, this proposal aims to coherently transfer atom pairs into their molecular ground state. Coherent transfer techniques are chosen for highly efficient conversion from one quantum state to another.

As a pre-requisite, the individual atoms have to be brought under full quantum control, including their motional degrees of freedom, which we achieved recently [5, 41] and described in the previous subsection. To overcome technical challenges associated with converting an atom pair to the ro-vibrational ground state of a molecule with a large energy difference but small wavefunction overlap, two steps (Fig. 2 and 9) are planned. A sodium and a cesium atom in the same tweezer will first be associated into the most weakly bound molecular state (vibrational level $\nu'' = 24$ in $a^3\Sigma^+$) by a detuned, coherent, two-photon Raman pulse (Fig. 9A). We have performed a detailed calculation that shows the transfer process could be as efficient as 98% [41].

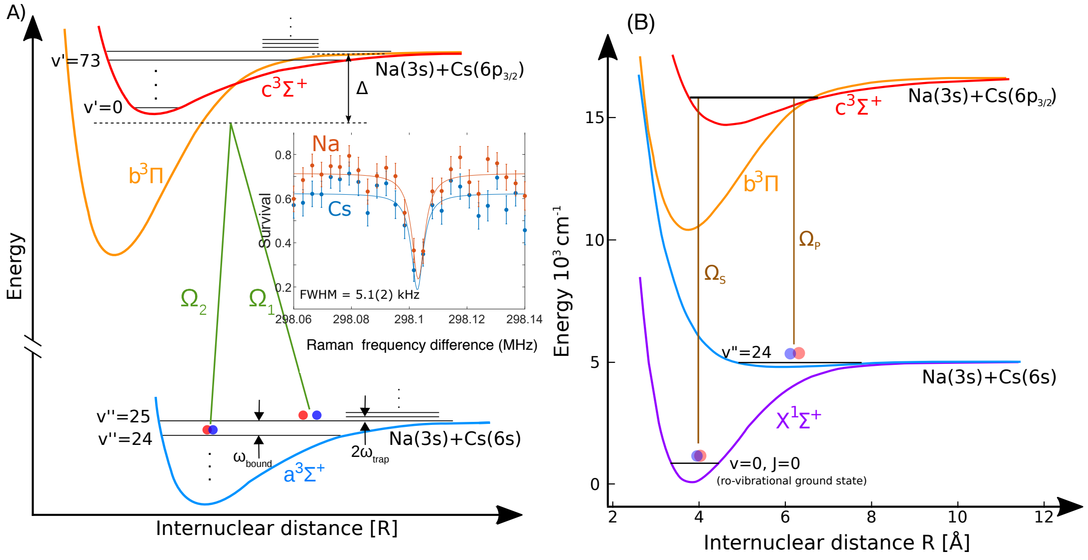

FIG. 9. Schemes for two-step coherent conversions of an atom pair into the absolute rovibrational ground state of NaCs. (A) A detuned two-photon Raman scheme for converting the atom pair in $v'' = 25$ to the least-bound molecular state $v” = 24$ of $a^3\Sigma^+$. Inset, preliminary data showing atoms transferred into the $v” = 24$ level at a binding energy of 298.1 MHz. The transfer is manifested as simultaneous loss of a Na and a Cs atom. (B) A STIRAP scheme to convert weakly-bound molecules from $v” = 24$ of $a^3\Sigma^+$ to $v” = 0$ of $X^1\Sigma^+$. The up leg and down leg transitions are around 920 nm and 633 nm respectively.

To associate the atoms into the loosely-bound molecular state, we use a two-photon Raman pulse between the trap ground state and the loosely-bound molecular state ($a^3\Sigma$, $v'' = 24$), as shown in Fig. 9(A). A two-photon Raman pulse requires an intermediate excited state with good wavefunction overlap between both ground states. Theoretical simulations of the Raman transfer process predict that the lowest vibrational level ($v' = 0$) of the excited molecular state $c^3\Sigma$ gives optimum transfer efficiency. We conducted spectroscopy of the $c^3\Sigma$ state with a photoassociation pulse and looked for simultaneous loss of both Na and Cs atoms, and observed the lowest vibrational state at 288694 GHz.

We then used this $c^3\Sigma$ $v' = 0$ excited state to perform EIT (electromagnetic-induced transparency) between the trap ground state and the loosely bound molecular state, as shown in the caption of Fig. 9(A). When the detuning of the two lasers matches the binding energy of the loosely bound state, then a transparency window prevents photoassociation, and we detect less two-body loss. We measured the binding energy of the loosely bound molecular state to be 297.8(1) MHz.

We then attempted to perform a coherent transfer between the two ground states. At first, efficiency of the transfer process was low, and we discovered the cause waslarge off-resonant scattering of the loosely bound molecular state due to the tweezer light. To overcome this problem, we redesigned our tweezer setup so that the tweezer light is the same frequency as what we need for the Raman transfer, $\sim$ 1038 nm. Using the tweezer light for the Raman transfer, we observed 20% coherent oscillations between the atoms in the trap ground state to the loosely bound molecular state.

The contrast of the Rabi oscillations suggest that only 20% of the initial atoms are being converted to molecules. One likely explanation for the low conversion is that the loosely bound molecule state we are driving to might have a different parity from the initial atoms, for example if it has rotational angular momentum. We are currently performing spectroscopy on the loosely bound state to locate the three predicted rotational states.

Subsequently, the weakly-bound ($\nu'' = 24$) molecule will be transferred into the rotational, vibrational, and electronic (rovibronic) ground state by STImulated Raman Adiabatic Passage (STIRAP) [37] (Fig. 9B). We expect the STIRAP process to have an efficiency $> 95\%$. For the technical implementation, we plan to frequency stabilize the STIRAP lasers (633 nm and 920 nm) to a high-finesse cavity. Spectroscopy search of relevant NaCs excited and ground states will also be necessary. Once we perfect the steps of making one ground-state molecule from two atoms, we will extend the system to an array of molecules by scaling up the number of optical tweezer atom traps in the first step of molecular assembly. In Fig. 2, we show a preliminary effort - an array of 9 single Cs atoms in optical tweezers, generated by driving acoustic-optical deflectors with multiple frequency tones. We plan to also extend the number of optical tweezers for Na atoms and demonstrate real-time tweezer re-arrangement with two different atomic species.

E. Theoretical investigation of high-fidelity quantum logic with polar molecules

Complimentary to our experimental work, we investigated the prospects of using our molecules for quantum computing. We proposed and analyzed a realistic, scalable scheme to implement two-qubit gates with molecules [12]. Our analysis shows that a high fidelity ($> 99.99\%$) can be achieved while the system can be scaled up by purely optical means. Our new findings indicate that molecules are indeed promising qubits.

Previous proposals consider simplified molecular structure, ignoring realistic constraints and requiring experimental fine-tuning to separate "degenerate" molecular levels [10, 11]. These can nullify the advantages of using molecules as nature's "pre-packaged" qubits in the first place. In our study, we consider the full molecular Hamiltonian for the specific example of NaCs molecules and use internal molecular coupling and intrinsic dipolar exchange interactions between molecules for the two-qubit gate scheme. Our scheme requires no additional large or extremely stable electromagnetic fields, and therefore preserves the molecules' intrinsic long coherence times. The interactions between molecules are toggled on and off by targeted light shifts and global microwave pulses. We analyze the two-qubit gates including experimental imperfections and the effects from the optical trapping and conclude that a fidelity$>$ 99.99% can be achieved. At the same time, we identify population leakage and recoil heating as important effects that must be controlled to achieve high fidelity.

We also envision future experimental work to make available a number of different molecular species for qubits for computing. Our scheme, concretely proposed for NaCs, can be generalized to other molecular species to take full advantage of the rich palette of molecular species and their long coherence times.

V. CONCLUSIONS

In conclusion, we have developed a set of tools for manipulating a *general* class of atomic species for ultracold molecular assembly, demonstrated here on Na and Cs atoms. These include single atom loading, trapping and imaging in optical tweezers [29]; control of the motional degree of freedom down to a single quantum state [40,41]; persistence of this single motional quantum state despite transporting the atom over large distances; "handing off" of a single atom between separate optical tweezers [36]; and on-demand chemical reactions and detailed collisional and spectroscopic studies between exactly two atoms [36].

Our next efforts, already under way, are two-fold: 1) theoretical and spectroscopic study of the structure of the NaCs molecule to complete the transfer to the desired molecular state; and 2) scaling up to large arrays of molecules.

Control over single molecules provides promise for a variety of modern technological challenges, including detailed understanding of chemical reactions, and building quantum computers and quantum simulators for materials science.

Nevertheless, the tools we developed should also be of general interest to the burgeoning community of single-atom trappers. We envision that these tools will become enabling, and eventually standard, techniques in the ongoing push to bring more atomic and molecular species under optical tweezer control.

[1] N. Schlosser, G. Reymond, I. Protsenko, and P. Grangier, Nature **411**, 1024 (2001).

[2] N. R. Hutzler, L. R. Liu, Y. Yu, and K.-K. Ni, New Journal of Physics **19**, 023007 (2017).

[3] A. M. Kaufman, B. J. Lester, and C. A. Regal, Phys. Rev. X **2**, 041014 (2012).

[4] J. D. Thompson, T. G. Tiecke, A. S. Zibrov, V. Vuletić, and M. D. Lukin, Phys. Rev. Lett. **110**, 133001 (2013).

[5] Y. Yu, N. R. Hutzler, J. T. Zhang, L. R. Liu, J. D. Hood, T. Rosenband, and K.-K. Ni, Phys. Rev. A **97**, 063423 (2018).

[6] L. R. Liu, J. D. Hood, Y. Yu, J. T. Zhang, N. R. Hutzler, T. Rosenband, and K.-K. Ni, Science **360**, 900 (2018), http://science.sciencemag.org/content/360/6391/900.full.pdf.

[7] R. V. Krems, Physical Chemistry Chemical Physics **10**, 4079 (2008).

[8] M. A. Baranov, M. Dalmonte, G. Pupillo, and P. Zoller, Chemical Reviews **112**, 5012 (2012),

pMID: 22877362, http://dx.doi.org/10.1021/cr2003568.

[9] A. Aspuru-Guzik, A. D. Dutoi, P. J. Love, and M. Head-Gordon, Science **309**, 1704 (2005), http://science.sciencemag.org/content/309/5741/1704.full.pdf.

[10] .

[11] S. F. Yelin, K. Kirby, and R. Côté, Phys. Rev. A **74**, 050301 (2006).

[12] K.-K. Ni, T. Rosenband, and D. D. Grimes, Chem. Sci. (2018 (in press)), 10.1039/C8SC02355G.

[13] A. Andre, D. DeMille, J. M. Doyle, M. D. Lukin, S. E. Maxwell, P. Rabl, R. J. Schoelkopf, and P. Zoller, Nat. Phys. **2**, 636 (2006).

[14] L. D. Carr, D. DeMille, R. V. Krems, and J. Ye, New Journal of Physics **11**, 055049 (2009).

[15] K.-K. Ni, S. Ospelkaus, M. H. G. de Miranda, A. Pe'er, B. Neyenhuis, J. J. Zirbel, S. Kotochigova, P. S. Julienne, D. S. Jin, and J. Ye, Science **322**, 231 (2008).

[16] J. G. Danzl, E. Haller, M. Gustavsson, M. J. Mark, R. Hart, N. Bouloufa, O. Dulieu, H. Ritsch, and H.-C. Nagerl, Science **321**, 1062 (2008), http://www.sciencemag.org/cgi/reprint/321/5892/1062.pdf.

[17] F. Lang, K. Winkler, C. Strauss, R. Grimm, and J. H. Denschlag, Phys. Rev. Lett. **101**, 133005 (2008).

[18] A. Chotia, B. Neyenhuis, S. A. Moses, B. Yan, J. P. Covey, M. Foss-Feig, A. M. Rey, D. S. Jin, and J. Ye, Phys. Rev. Lett. **108**, 080405 (2012).

[19] T. Takekoshi, L. Reichsöllner, A. Schindewolf, J. M. Hutson, C. R. Le Sueur, O. Dulieu, F. Ferlaino, R. Grimm, and H.-C. Nägerl, Phys. Rev. Lett. **113**, 205301 (2014).

[20] P. K. Molony, P. D. Gregory, Z. Ji, B. Lu, M. P. Köppinger, C. R. Le Sueur, C. L. Blackley, J. M. Hutson, and S. L. Cornish, Phys. Rev. Lett. **113**, 255301 (2014).

[21] J. W. Park, S. A. Will, and M. W. Zwierlein, Phys. Rev. Lett. **114**, 205302 (2015).

[22] M. Guo, B. Zhu, B. Lu, X. Ye, F. Wang, R. Vexiau, N. Bouloufa-Maafa, G. Quéméner, O. Dulieu, and D. Wang, Phys. Rev. Lett. **116**, 205303 (2016).

[23] S. Ospelkaus, K.-K. Ni, D. Wang, M. H. G. de Miranda, B. Neyenhuis, G. Quéméner, P. S. Julienne, J. L. Bohn, D. S. Jin, and J. Ye, Science **327**, 853 (2010), http://science.sciencemag.org/content/327/5967/853.full.pdf.

[24] B. Yan, S. A. Moses, B. Gadway, J. P. Covey, K. R. A. Hazzard, A. M. Rey, D. S. Jin, and J. Ye, Nature **501**, 521 (2013).

[25] S. A. Moses, J. P. Covey, M. T. Miecnikowski, D. S. Jin, and J. Ye, Nat Phys **13**, 13 (2017).

[26] B. Gadway and B. Yan, Journal of Physics B: Atomic, Molecular and Optical Physics **49**, 152002 (2016).

[27] J. Deiglmayr, M. Aymar, R. Wester, M. Weidemüller, and O. Dulieu, The Journal of Chemical Physics **129**, 064309 (2008), http://aip.scitation.org/doi/pdf/10.1063/1.2960624.

[28] P. J. Dagdigian and L. Wharton, The Journal of Chemical Physics **57**, 1487 (1972), http://aip.scitation.org/doi/pdf/10.1063/1.1678429.

[29] A. Grochola, P. Kowalczyk, J. Szczepkowski, W. Jastrzebski, A. Wakim, P. Zabawa, and N. P. Bigelow, Phys. Rev. A **84**, 012507 (2011).

[30] A. Wakim, P. Zabawa, and N. P. Bigelow, Phys. Chem. Chem. Phys. **13**, 18887 (2011).

[31] P. Zabawa, A. Wakim, M. Haruza, and N. P. Bigelow, Phys. Rev. A **84**, 061401 (2011).

[32] P. S. Żuchowski and J. M. Hutson, Phys. Rev. A **81**, 060703 (2010).

[33] N. Schlosser, G. Reymond, and P. Grangier, Phys. Rev. Lett. **89**, 023005 (2002).

[34] C. Monroe, D. M. Meekhof, B. E. King, S. R. Jefferts, W. M. Itano, D. J. Wineland, and P. Gould, Phys. Rev. Lett. **75**, 4011 (1995).

[35] X. Li, T. A. Corcovilos, Y. Wang, and D. S. Weiss, Phys. Rev. Lett. **108**, 103001 (2012).

[36] S. Grishkevich and A. Saenz, Phys. Rev. A **76**, 022704 (2007).

[37] K. Bergmann, H. Theuer, and B. W. Shore, Rev. Mod. Phys. **70**, 1003 (1998).

[38] See supplementary material.

[39] R. A. Cline, J. D. Miller, M. R. Matthews, and D. J. Heinzen, Opt. Lett. **19**, 207 (1994).

[40] J. D. Teufel, T. Donner, D. Li, J. W. Harlow, M. S. Allman, K. Cicak, A. J. Sirois, J. D. Whittaker, K. W. Lehnert, and R. W. Simmonds, Nature **475**, 359 (2011).

[41] L. R. Liu, J. T. Zhang, Y. Yu, N. R. Hutzler, Y. Liu, T. Rosenband, and K.-K. Ni, ArXiv:1701.03121 (2017), arXiv:1701.03121 [physics.atom-ph].